RETENTION CAPACITIES OF ZIRCONIA AND APATITES TOWARDS IODINE AND TECHNETIUM FISSION PRODUCTS

N. Millard-Pinard, F. Brossard, N. Chevarier, A. Chevarier, D. Crusset*
C. Gaillard, N. Moncoffre, K. Poulard
Institut de Physique Nucléaire de Lyon, IN2P3/CNRS, Université Claude Bernard, F-69622 Villeurbanne Cedex, France, e-mail : millard@ipnl.in2p3.fr
*ANDRA, Parc de la Croix Blanche, F-92298 Châtenay-Malabry Cedex, France.

ABSTRACT

This paper is devoted to the study of apatites and zirconia used as conditioning materials of nuclear wastes. Among the long-lived fission products ^{129}I and ^{99}Tc release has to be evaluated. First, the stable isotopes ^{187}Re and ^{98}Mo considered as chemical homologous of Tc were implanted in hydroxyapatite. Then, cladding tube pieces (hulls) present a thin superficial zirconia layer in which most of the radioactivity is concentrated. Stable ^{127}I release due to diffusion or to corrosion process was investigated in order to model its long term behaviour. Diffusion studies were performed by successive air annealings (300-900°C). The distribution evolution characterised by RBS allowed to identify the migration mechanisms. XPS and XANES methods were used to follow the chemical evolution of the compounds as function of temperature.

Keywords : Zirconia, apatites, fission products, diffusion, corrosion

1- INTRODUCTION

This paper presents a synthesis of different studies performed in our laboratory and which concern the geological disposals of medium and high-level activity nuclear wastes containing long-lived radionuclide elements [1,2,3]. Among them, we have focused our interest on high radiotoxicity fission products which release has to be evaluated. These elements are ^{129}I ($T=16\times10^6$ years) which is known to be very volatile and ^{99}Tc ($T=2\times10^5$ years) which oxides are also volatile. Indeed this study was performed using the stable isotopes 127 iodine and, molybdenum 98, and rhenium 187 considered as a chemical homologous of technetium. Two materials were more particularly studied:

First, apatites whose general formula is $Ca_{10}(PO_4)_6X_2$, X being a fluorine, chlorine ion or an hydroxyl group. This material has a strong ability to incorporate a wide range of elements in its crystalline structure [4,5]. It is therefore studied in order to be introduced either into waste containers as filling material or into concrete structures surrounding the containers. In this paper, we present a study on the migration mechanisms of Mo and Re induced by air annealing.

Second, hulls which are pieces of cladding tubes obtained after reprocessing. During Pressurised Water Reactor operation, the cladding tubes get oxidised on both the inner side and the external side. The external oxidation of about 100 µm thickness is due to the contact with the cooling water and has been largely studied. The internal oxidation due to the contact with the UO_2 fuel is much thinner (about 10 µm) and has been rarely taken into account [6]. During reprocessing the cladding tubes are cut up and washed with nitric acid to dissolve the spent fuel. Considering that fission products are implanted by recoil in this oxide layer and remain implanted in the hulls even after reprocessing, it is important to study the dissolution of this zirconia layer in the hypothesis of a geological disposal. Results concerning hulls will be split into two parts. A thermal migration study of I in zirconia and a simulation of corrosion in severe pH conditions. This last part is essential since hulls were embedded in concrete until 1995 and concrete barriers will be very likely used as last barriers in geological disposals.

2- THERMAL MIGRATION UNDER DRY AIR ANNEALING

2-1. Migration study by coupling ion implantation and RBS profiling

Iodine, molybdenum and rhenium were introduced in the studied materials by ion implantation. The samples were then annealed in air at high temperature (300-900°C) in order to accelerate the migration processes. After

each annealing step, the profile evolution was followed by RBS which allows to obtain information on the I, Mo, and Re migration mechanisms.

The initial profile of the as implanted samples is very close to a Gaussian distribution :

$$C(x,t=0) = \frac{N_{impl}}{\sqrt{2p}\,\Delta R}\exp\left[-\frac{(x-R)^2}{2\Delta R^2}\right] \qquad (1)$$

where $C(x\ t=0)$ is the initial ion concentration, x the distance from the implanted surface, N_{impl} the implanted ion dose, R the mean range of the Mo, Re or I ions and DR the range straggling.

The gaussian distribution can evolve with time according to three independent processes, whose effects on a gaussian distribution are resumed on figure 1.

i) Diffusion can be induced by the concentration gradient of the element. It implies a broadening of the distribution which tends to an uniform concentration over depth.

ii) The particle movement in a given direction is due to an external force, or driving force, which involves a shift of the atoms towards a x direction with a force U. In our experiments, the driving force corresponds to a chemical potential gradient in the sample and leads to a shift of the whole distribution towards the surface.

iii) The loss of matter traduces an instant volatilisation of the element, with a release coefficient k. It appears through a global decrease of the species concentration, without any broadening of the distribution.

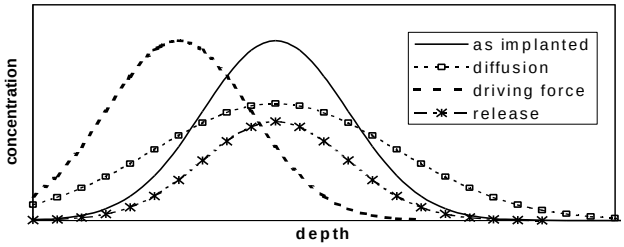

Figure 1: Effect of diffusion, driving force towards the surface and matter release

on the profile evolution of implanted species

Those processes are independent but they can happen simultaneously. In this case, the global evolution of the species concentration C with time is given in equation 2:

$$\frac{\P C}{\P t} = D\frac{\P^2 C}{\P x^2} + U\frac{\P C}{\P x} - k.C \qquad (2)$$

where D is the diffusion coefficient, U is the driving force and k is the release coefficient.

In the present experiments, the species evolution was due at maximum to two processes at the same time (diffusion/matter loss or driving force/matter loss).

2-2. Experiment

2-2a. Sample preparation

Apatite

Experiments were performed on synthetic microcrystalline hydroxyapatite, referenced as DNA grade Bio-gel HTP, stacked into pellets at 0.4 GPa. The high crystallinity was confirmed by X-ray diffraction. Structural observations by scanning electron microscopy showed a high density of grain boundaries with sizes less than 10 nm.

Zirconia

The samples used in the experiments were obtained by annealing pure polycrystalline zirconium under atmospheric pressure at 500°C for 3 hours. The zirconia layer was characterised by Scanning Electron Microscopy (SEM) and RBS. SEM data obtained on a slant cut sample showed that the layer is homogeneous but the ZrO_2/Zr interface is not sharp. These observations were confirmed by 3 and 7.5 MeV alpha backscattering measurements. The zirconia layer thickness deduced from RBS is 1.3± 0.2 µm which is much larger than the implantation depth. Moreover a quite broad interface, around 0.3 µm thick, was observed. It is characteristic of the substoichiometric oxide growth at this interface.

2-2b Profiling

For RBS experiments, the depth resolution was optimised in order to measure precisely ^{127}I, ^{98}Mo and ^{187}Re evolution profiles. The implantation energies (between 100 and 200 keV) were thus chosen so that the ranges were the same (about 50 nm). Due to the sensitivity of the technique, we adopted a 1×10^{16} at cm^{-2} dose.

The apatite samples were annealed in air between 300 and 550°C for molybdenum implanted samples and between 450 and 550°C for rhenium implanted samples. The higher temperature was limited to 550°C since hydroxyapatite begins to decompose above this temperature. In case of iodine in zirconia, the annealing temperature was varied between 600 and 900°C.

RBS results are presented in figures 2a, 2b, 2c corresponding respectively to Mo, Re and I RBS profiles.

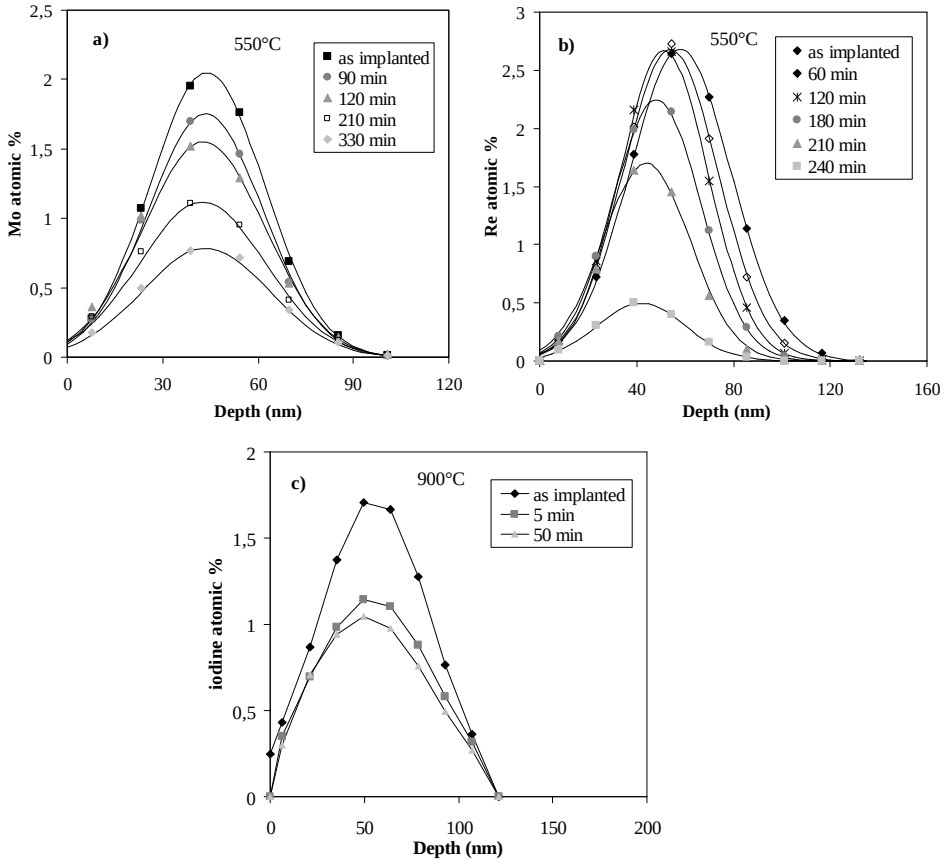

Figure 2: Evolution of a) molybdenum b) rhenium and c) iodine depth distributions as function of annealing time at 550°C and 900°C. The numerical fits are represented by full lines.

Another way to present these results is to plot the release percentage of the implanted elements as function of annealing time. The release rates are deduced directly from the profile integration over depth for each annealing time. Such a representation is given in figure 3.

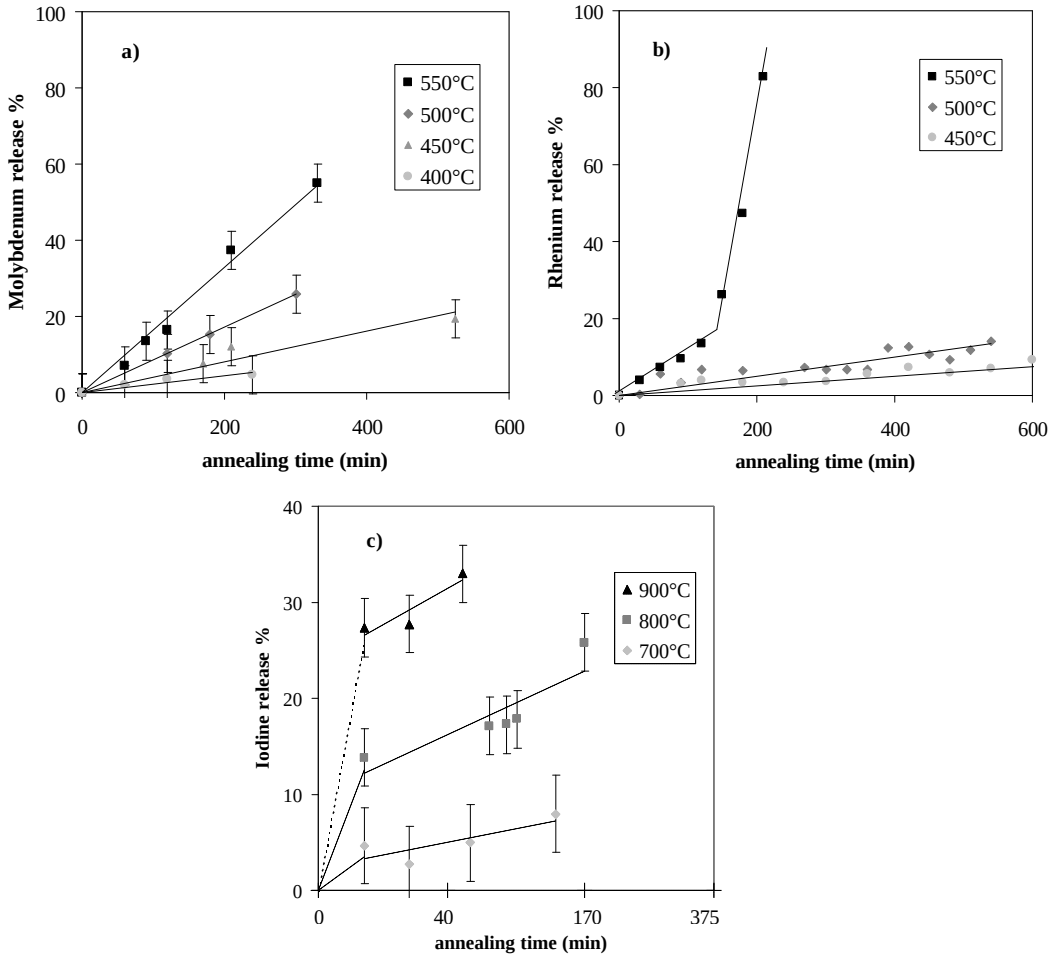

Figure 3 : Evolution of a) molybdenum b) rhenium and c) iodine release versus annealing time at different temperatures

Let us consider from figure 2, the profile evolution for each element. For molybdenum, no profile shift is noted and a profile broadening cannot be easily observed, implying that the diffusion is not the dominant process. So, the molybdenum concentration evolution with annealing time is on the form:

$$\frac{\partial C}{\partial t} = D\frac{\partial^2 C}{\partial x^2} - kC \qquad (3)$$

For rhenium, we can observe a slight shift towards the surface and a global decrease of the concentration. So, the evolution of rhenium concentration with annealing time can be written :

$$\frac{\partial C}{\partial t} = U\frac{\partial C}{\partial x} - k.C \qquad (4)$$

In case of iodine two phases can be observed: a very strong iodine release at the very beginning of the annealing procedure. We have shown [2] that this rapid phase depending on the iodine concentration and the zirconia structure is analogue to the release of volatile fission products observed during reactor processing. Therefore we analysed the profile evolution after the first 5 minutes of annealing in term of diffusion:

$$\frac{\partial C}{\partial t} = D\frac{\partial^2 C}{\partial x^2} \qquad (5)$$

Equations (3) ,(4) and (5) were solved taking as initial conditions the as-implanted distribution (equation (1)) and as boundary condition, we considered a semi-infinite medium : $C(\infty,t)=0$.

Evermore, in the case of equations (3) and (5), we have considered a boundary condition on the surface concentration:

$$D\frac{\partial C(0,t)}{\partial x} = K.C(0,t)$$

where K is the surface transparency. The diffusion coefficient is very small, implying that the surface concentration is small as it is experimentally observed**.**

Equations (3) , (4) and (5) were normalised using dimensionless variables [1], and solved by using a numerical approach, based on finite difference methods, fully described in ref [7]. The fits thus obtained are represented by full lines in figure 2.

The so deduced diffusion coefficients obtained for iodine and molybdenum are presented in table 1.

Iodine in zirconia		Molybdenum in apatite	
Annealing temperature	D ($cm^2\ s^{-1}$)	Annealing temperature	D ($cm^2\ s^{-1}$)
900°C	$5.6 \pm 0.2.10^{-16}$	550°C	$(1.8 \pm 0.6)\ 10^{-17}$
800°C	$2.0 \pm 0.5.10^{-16}$	500°C	$(5.5 \pm 2.3)\ 10^{-18}$
700°C	4 ± 2.10^{-17}	450°C	$(2.5 \pm 1.7)\ 10^{-18}$

Table 1: Iodine and molybdenum diffusion coefficients deduced from the fits of profile evolutions

From the Arrhenius law, it was possible to determine respectively an activation energy for iodine diffusion in zirconia equal to 1.1 ± 0.3 eV at^{-1} and an activation energy for molybdenum diffusion in apatite equal to 0.9 ± 0.2 eV at^{-1}.

The extrapolation to storage conditions (50°C) leads to a diffusion coefficient around 10^{-26} $cm^2\ s^{-1}$ in both cases which proves that the diffusion mechanism cannot be responsible for significant releases.

From the depth distribution and release rate analysis we deduced the Mo and Re release factors k. The results are presented in table 2.

Annealing temperature (°C)	k (s^{-1}) for Mo	k (s^{-1}) for Re
450	$(7.0 \pm 2.1)\ 10^{-6}$	$(1.7 \pm 2.1)\ 10^{-6}$
500	$(1.6 \pm 0.3)\ 10^{-5}$	$(3.7 \pm 0.3)\ 10^{-5}$
550	$(4.1 \pm 1.0)\ 10^{-5}$	$(2.0 \pm 1.0)\ 10^{-5}$ $(4.0 \pm 0.5)\ 10^{-4}$

Table 2: Molybdenum and Rhenium release coefficients k deduced from the release rates.

The Arrhenius plot corresponding to the release coefficients of table 2 allows to deduce release activation energies. They are respectively equal to 0.7 eV at^{-1} for Mo and 1.2 eV at^{-1} for Re. Those values indicate that the Mo release is energetically easier than the Re one. Those elements are not volatile in the studied temperature range, which means that their volatilisation is due to the formation of volatile compounds that we have tried to put in evidence by a chemical characterisation.

2-3. Mo and Re chemical characterisation

RBS analysis put in evidence a volatilisation of molybdenum and rhenium. This loss is not the consequence of diffusion or of a driving force. We also put in evidence by annealing under primary vacuum (10^{-2} mbar) that the release rate depends on the amount of oxygen in the annealing atmosphere [8]. Therefore, in order to understand the mechanisms responsible for the volatilisation, we carried out chemical analysis of molybdenum and rhenium. These studies were made on samples annealed at 300°C for which no release could be observed, so that we would follow the formation of the volatile species.

X-ray Photoelectron Spectroscopy (XPS) analysis provides the oxidation degree evolution of rhenium and molybdenum at the very near surface (5 nm). Moreover, X-ray Absorption Near-Edge Spectroscopy (XANES) studies gave us information on the structure of the compounds formed during annealing. The detection modes were chosen in order to probe either the whole implanted depth (150 nm) or only part of it (50 nm). For example,

we have chosen fluorescence detection in the analysis of XANES spectrum at the molybdenum K edge in order to have representative information on the total implanted depth while we used the total electron yield mode in the analysis of XANES spectrum at the molybdenum $L_{II,III}$ edges which probes the first 50 nm of the samples. The results are summarised in figure 4.

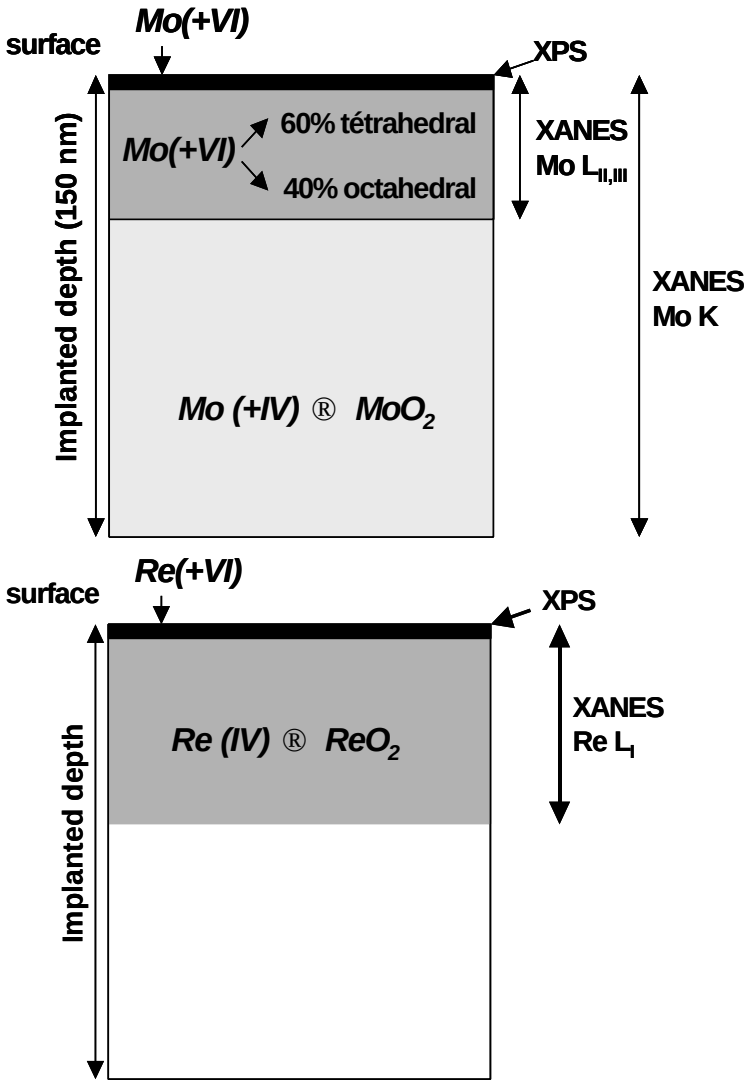

Figure 4: Chemical evolution of molybdenum and rhenium during annealing from XPS and XANES analysis.

These results put in evidence a Mo and Re oxidation gradient as a function of depth. For molybdenum, the first formed oxide is MoO_2, in which molybdenum has a (+IV) oxidation degree and an octahedral co-ordination. With time, this oxide transforms to a Mo (+VI) compound in which molybdenum has two types of symmetry, octahedral and tetrahedral.

The first rhenium oxide showed by XANES is ReO_2. Considering that it evolves to a Re (+VI) compound, we can assume that it oxidises with time to ReO_3. This oxide is not volatile at the studied annealing temperatures. The most volatile rhenium oxide is Re_2O_7, where rhenium has a (+VII) oxidation degree. The fact that this compound is very volatile (above 250°C) may explain that even at 550°C we have not found any Re (+VII) species in our samples. Re_2O_7 probably volatilises as soon as it is formed.

The molybdenum and rhenium oxidation is tied to the presence of oxygen in the annealing atmosphere. So, it is correlated to the oxygen diffusion in the samples.

3. MIGRATION IN CORROSIVE MEDIUM

Corrosion tests were performed in autoclave. The specimens were exposed to a 300°C basic solution under a 140 bars pressure. The basic solution was representative of infiltrated water though a concrete media. This solution was prepared with sodium hydroxide (2.867 g/l) and potassium hydroxide (16.830 g/l). The resulting pH of this solution at 25°C was 13.5. The corrosion tests were conducted during 12 weeks with regular samplings every two weeks. During the contact between zirconia and the corrosive water, two phenomena can happen: a dissolution of the material surface and a migration of iodine. In order to follow the zirconia dissolution, we used europium as a surface marker and followed its evolution by RBS. The results obtained have allowed to determine a dissolution rate of zirconia of 1 nm per day [3].

As well, the iodine migration was studied by RBS profiling. The iodine profile evolution is given in figure 5 for the 14 and 28 days corrosion times in comparison with the as-implanted sample. In the first 14 days the iodine release reaches 80% and then remains stable [9]. Since the iodine loss is not related to the zirconia dissolution, its origin can correspond i) to an enhanced diffusion or ii) to the formation of a volatile compound, containing potassium or sodium for example, which would dissolve in the solution or iii) to an ion exchange process I^-/OH^-. By comparison of these results with iodine diffusion data in zirconia we can extrapolate an apparent diffusion coefficient of $2x10^{-29}$ cm^2 s^{-1} at 300°C. Considering this value, the diffusion phenomenon cannot explain the observed rapid iodine release. Since PIXE experiments did not allow to detect the presence of K or Na species on the sample surface, the formation of soluble KI or NaI compounds is unlikely. The last hypothesis of ion exchange in the basic medium very rich in OH^- species seems to be the most probable explanation. Recent hydrogen analysis experiments, not presented here, using Elastic Recoil Detection Analysis (ERDA) tend to prove that a hydrogen enrichment occurs at the sample surface as the duration stay of the samples in autoclave increases. Similar experiments are now being performed with pure water in order to confirm this hypothesis.

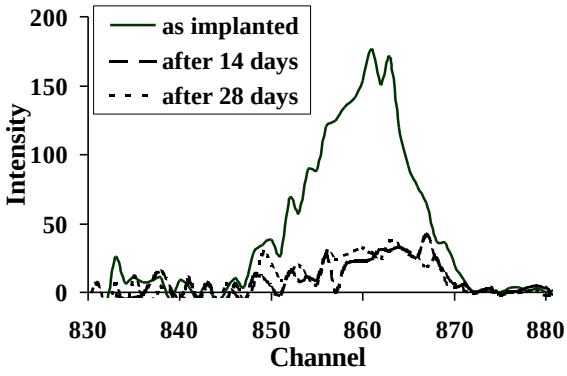

Figure 5: Evolution of the iodine concentration profiles at 300°C as function of the annealing time in autoclave.

4. CONCLUSION

The experiments on iodine migration in zirconia were made in order to analyse the mechanism of iodine release from hulls. We have identified two phases: A rapid release phase which was shown to disappear as far as the reorganisation of the zirconia structure occurs and a slow release correlated to a diffusion process. The extrapolation to waste disposal conditions leads to a negligible diffusivity. The experiments on Mo and Re migration were made in order to extrapolate on the technetium migration behaviour in apatite. They showed that the Mo and Re behaviours are led by the formation of oxidised volatile species. Since rhenium is the chemical analogue of technetium, we can assume that the Tc release will be also governed by its oxidation in Tc_2O_7, volatile at ambient temperature.

Concerning the corrosion experiments on iodine implanted zirconia, it appears that the enhanced iodine release is very likely due to an ion exchange I^-/OH^- and is not correlated to the matrix dissolution.

REFERENCE

[1] - C. GAILLARD, N. CHEVARIER, N. MILLARD-PINARD, P. DELICHERE, Ph. SAINSOT, ”Thermal diffusion in apatite”, Nucl. Instr. And Meth. In Phys. Res. B, 646, 164 (2000)

[2] - F. BROSSARD, N. CHEVARIER, N. MONCOFFRE, Ph. SAINSOT, D. CRUSSET, H. JAFFREZIC, ”Thermal iodine release of surface-implanted iodine in zirconia and its affect on hull disposal”, J. Nucl. Mater. 279, 153 (2000)

[3] - K. POULARD, A. CHEVARIER, J. C. DUCLOT, N. MONCOFFRE, D. CRUSSET, ”Use of RBS to validate europium surface implantation as a marker for the corrosion study of zirconia”, Nucl. Instr. and Meth. In Phys. Res. B, 668, 161 (2000)

[4] - J. CARPENA, J-L. LACOUT, ”Des apatites naturelles aux apatites synthétiques”, L’Actualité Chimique, 2, 3 (1997)

[5] - P. MARTIN, G. CARLOT, A. CHEVARIER, C. DEN AUWER, G. PANCZER, ”Mechanisms involved in thermal diffusion of rare earth elements in apatites”, J. Nucl. Mater., 275, 268 (1999)

[6] - H. KLEYKAMP, ”Post-irradiation examinations and composition of the residues from nitric acid dissolution experiments of high-burnup LWR fuel”, J. Nucl. Mater., 171, 181 (1990)

[7] - J. CRANK, The Mathematics of Diffusion, 2nd ed., Claredon, Oxford (1975)

[8] - C. GAILLARD, ”Etude de la migration thermique des produits de fission molybdène, technétium et iode dans les apatites”, Thesis, Claude Bernard University, Lyon 1, France (2000)

[9] - K. POULARD, A. CHEVARIER, N. MONCOFFRE, P. TROCELLIER, D. CRUSSET ”Study of Zircaloy-4 fuel cladding corrosion using ion beams - Application to long term disposal of nuclear wastes”, to be published in Nucl. Instr. And Meth. In Phys. Res. B